

Locally resonant acoustic metamaterial panels: 3D versus 2D modelling approaches

Henok Abadi

Eindhoven University of Technology

h.abadi@student.tue.nl

ABSTRACT

Locally resonant acoustic metamaterial (LRAM) panel designs have been regarded as potential solutions to attenuate flexural waves in lightweight (mostly thin) structures. Two-dimensional (2D) simplification modeling is often adopted for reducing analysis cost of 3D LRAM panels with consistent cross-sections along the width direction, based on the infinite width assumption. The applicability of such reduction strategy are evaluated in details. Comparative analyses between 3D and 2D modeling are carried out on a typical LRAM panel design. The results suggest the unit cell width-to-length ratio to be over 10 for applying the dimensionality reduction approach.

Keywords

Locally resonant acoustic metamaterial panel, band gap, dispersion analysis, frequency response analysis.

INTRODUCTION

For environmental and economic reasons, lighter but also stronger designs are constantly pursued in the modern society [1]. Various lightweight designs have emerged and received great successes. For example, the use of aluminum-based designs is helping in vehicle weight reduction, thereby improving the fuel economy. However, most of the lightweight designs consist of thin structures, of which the innate high stiffness to mass ratio leads to poor performance in the noise and vibration isolation aspects [2]. Such disadvantages become even more notable in the low-frequency regime.

The low-frequency vibration behaviors of thin structures is mainly dominated by the flexural (bending) wave and can induce substantial structural distortions on thin structures. For instance, lightweight wooden floors are used because of their sustainability and ease of construction, a disadvantage of these floors is the low acoustic performance. Impact sound transmission at low frequencies is caused by footsteps or machinery's (e.g. washing machine) [3]. To attenuate flexural waves and meanwhile keep lightweight, locally resonant acoustic metamaterial (LRAM) panel designs are being considered as potential solutions by benefiting from the unusual negative mass or modulus effects [4]. Different LRAM panels have shown capabilities to open the band gaps (frequency ranges in which waves cannot propagate) for the subwavelength flexural waves, while not needing large dimensions [see Figure 1(a)].

*Permission to make digital or hard copies of all or part of this work for personal or classroom use is granted under the conditions of the Creative Commons Attribution-Share Alike (CC BY-SA) license and that copies bear this notice and the full citation on the first page**

Many LRAM panels have consistent cross-section configurations along the width direction. For reducing analysis cost, two-dimensional (2D) simplification under the infinite width and thereby plane strain state assumption is often employed. In this case, only the along-length wave propagation is considered [see Figure 1(b)]. However, realistic LRAM panels must have finite sizes and boundary conditions along the width direction can be arbitrary, which may break the mentioned dimensionality reduction assumption. These issues place a clear need on evaluating the applicability of 2D simplification.

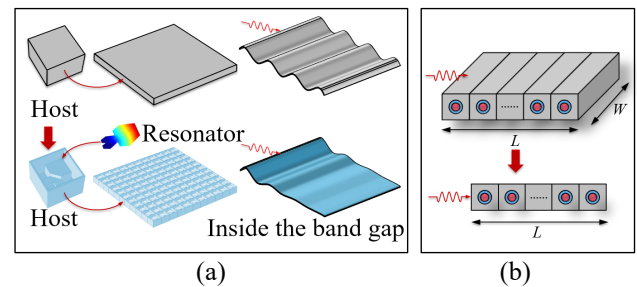


Figure 1: (a) improvement on the structural wave attenuation performance by replacing the conventional thin (host) panel by LRAM panel, based on a practical design in [5], and (b) reduction from 3D to 2D modelling.

This contribution thereby aims at examining if the dimensionality reduction approach is reasonable and also identifying its applicable conditions. These goals are achieved through comparative numerical investigations on 3D and corresponding simplified 2D models of a typical LRAM panel design using COMSOL Multiphysics. For generality, both dispersion and frequency response analyses are carried out, responsible for the infinite and finite cases, respectively.

NUMERICAL INVESTIGATIONS ON INFINITE LRAM PANELS

Modeling approaches

An infinitely long LRAM panel is considered first, which is periodically constructed by unit cells, as sketched in Figure 2(a). The 3D unit cell design is extruded from the typical 2D design in [6], as shown in Figure 2(b). The unit cell takes a classical negative mass design consisting of the matrix, coating and core constituents [7]. Since the focus is on low-frequency vibration resistance of the lightweight structures, the matrix material is selected as stiff and light as possible, e.g. glass while the coating material as soft as possible, e.g. rubber and core as heavy as possible, e.g. the tungsten. Corresponding material properties are collected in Table 1. In this unit cell, matrix: external length $L_m = 10.0$ mm, external thickness $H = 8.00$ mm, coating:

external length $l = 5.00$ mm, external thickness $h = 3.00$ mm, notch size $w = 0.500$ mm and external boundary of the core is geometrically similar to that of the coating, with a scaling factor 0.5. In the following, Finite element method (FEM) is employed for numerical analysis. A set of linear hexahedral elements are used to discretize the unit cell domain, with the cross-section element size ranging 0.1 to 0.5 mm and along-width element size 1.00 mm. Through the eigenmode analysis under the free boundary conditions (not displayed), the present mesh has been confirmed as able to yield the converged solutions.

Table 1: Material properties of adopted LRAM unit cell constituents (E : Young's modulus, ν : Poisson's ratio, ρ : mass density).

Material	E	ν	ρ
Glass matrix [8]	107 GPa	0.279	$2.05 \cdot 10^3$ kg/m ³
Rubber coating [9]	35 KPa	0.469	$1.30 \cdot 10^3$ kg/m ³
Tungsten core [10]	411 GPa	0.280	$1.92 \cdot 10^4$ kg/m ³

By applying Bloch periodic boundary conditions to the unit cell [11], the wave propagation analysis on the infinite LRAM panel can be reduced as the dispersion analysis on its unit cell. Solving the eigenvalue problems under a series of wave number finally yields the dispersion spectrum. Band structure calculations are evaluated for the wave vector components along the boundary of the first irreducible Brillouin zone Γ - X - M , see, e.g., [10] for details. The dispersion spectrum visualises the relation between the frequency and wavenumber.

For generality, dispersion analyses in a range of 0-1000 Hz are carried out under three different along-width boundary conditions: fixed ($u_z = 0$), free and 3) Bloch periodicity. For all cases the top and bottom boundaries are traction-free and Bloch periodic boundary conditions are applied to the two side boundaries to model wave propagation in the length direction. The width W_m is varied from $W_m = L_m$ to $10L_m$, in order to evaluate the applicability of 2D simplification.

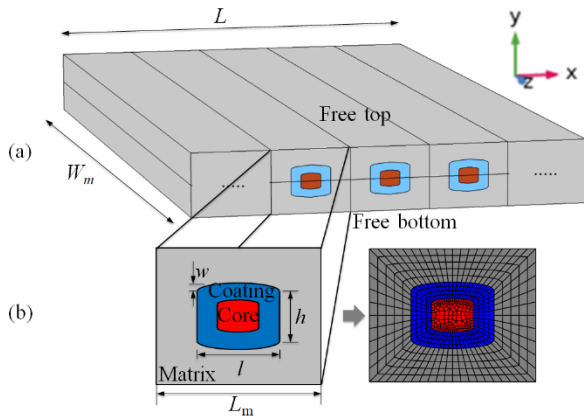


Figure 2: (a) an infinitely long 3D LRAM panel, and (b) unit cell dimensions and generated mesh.

Results

Dispersion analysis

The dispersion spectra of adopted 3D LRAM panel with $W_m = 10L_m$ for fixed, Bloch periodic and free boundary conditions are compared in Figures 3(a), 3(b) and 3(c) respectively. A flexural wave band gap can be clearly noticed as existing from 494 Hz to 635 Hz, which is in fact opened by the coupling effect of the out of plane inclusion linear motion. The localized rotational mode at 403 Hz exerts no influence on opening the flexural wave band gap. In comparison, the dispersion spectrum under the free boundary conditions show many more wave branches, since waves can propagate in the width direction.

Next, the dispersion spectra of 3D LRAM panel under different along-width boundary conditions are compared with that using 2D simplification modelling, as shown in Figure 4(a). For the purpose of reference, 2D localized mode shapes are also given, as shown in Figure 4(b). It can be found that for fixed and Bloch periodic boundary conditions the band gap size and position is identical to the 2D unit cell case, for free boundary conditions the band gap position is nearly identical with a deviation under 1%, the size is similar. As expected, when fixed boundary conditions are used the dispersion spectrum is identical to the 2D LRAM panel. Because the width direction is fixed the same plane strain state as in the 2D LRAM panel applies. Hence, the size of the width has no influence on the dispersion spectrum.

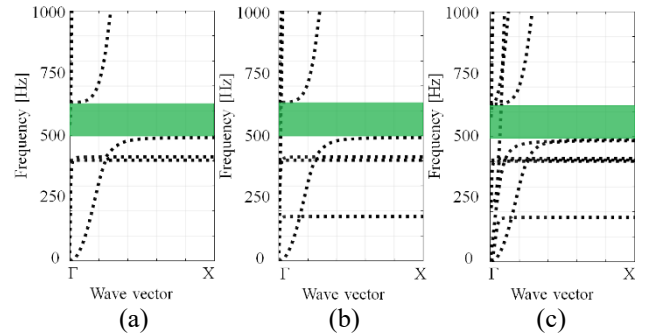


Figure 3: The dispersion spectra of the infinitely long 3D LRAM panel under the (a) fixed boundary conditions, (b) Bloch periodic boundary conditions and (c) free boundary conditions.

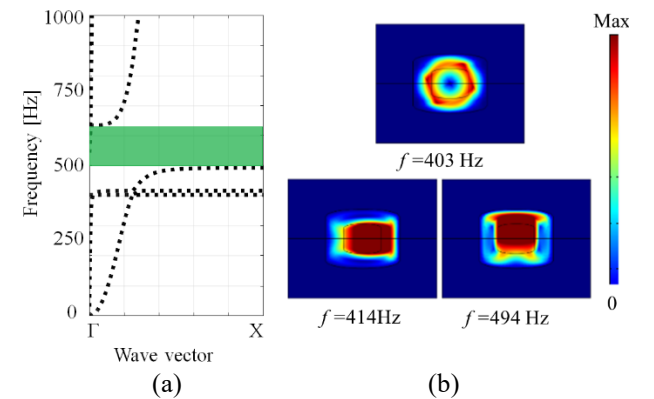


Figure 4: The (a) dispersion spectrum of the infinitely long 2D LRAM panel by dimensionality reduction, and (b) localized mode shapes.

In order to evaluate the applicability of 2D simplification, Figure 5 displays the upper and lower boundaries of the band gap for the three boundary conditions as function of the unit cell width-to-length ratio W_m/L_m , together with the 2D LRAM panel result. As the width becomes larger plane strain state is approached and the band gap for the free boundary condition shifts to higher frequencies and converges with the 2D LRAM panel band gap. With an increase of the width the boundary reflection effects that cause interference of the wave propagation decrease. As expected, for fixed and Bloch periodic boundary conditions the band gap is identical to the 2D LRAM panel band gap, independent of width.

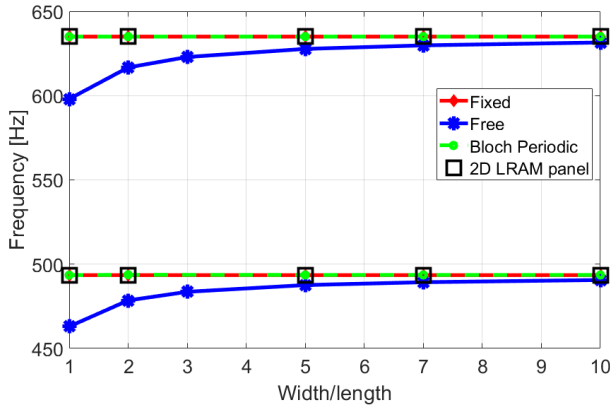


Figure 5: Band gaps of the infinitely long 3D LRAM panel under three different boundary conditions and 2D LRAM panel, with respect to the unit cell width to length ratio W_m/L_m .

It can be concluded that for a 3D LRAM panel with an unit cell width-to-length ratio W_m/L_m of at least 10 the dimensionality reduction approach is sufficiently accurate since the size and position of the flexural wave band gap is nearly identical between 3D and 2D LRAM panels for fixed, Bloch periodic and free boundary conditions.

NUMERICAL INVESTIGATIONS ON FINITE LRAM PANELS

Modeling approaches

To validate the conclusions made in the previous section, frequency response analyses on the LRAM panel with finite length are carried out. The 3D LRAM panel consists of unit cells with width $W_m = 10L_m$, based on the width parameter study of the dispersion analyses. According to these analyses, at this width there are minimal differences in band gap size and position between the three previously discussed boundary conditions, this has been validated for the finite panel.

Similar to the dispersion analyses, the top and bottom boundaries are traction-free. On the left edge of the panel a transverse displacement excitation is prescribed on the complete edge (highlighted in green in Figure 6). The right end middle edge is fixed since the bending behaviour is of primary interest. Therefore, the LRAM panel needs to be appropriately thin and is consisting of

50 unit cells, the total length of the panel is $L_{tot} = 50L_m$ (500 mm).

Free boundary conditions are applied along-width and two gauge points are taken at $2/5$ and $4/5$ of the panel. The distance between a gauge point and excitation source is noted as the x-coordinate difference.

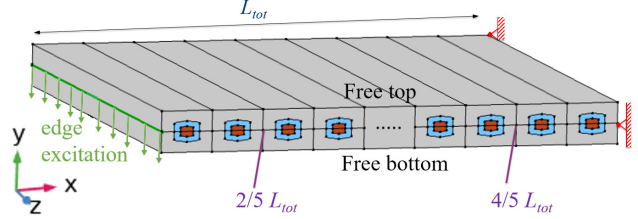


Figure 6: A finitely long 3D LRAM panel consisting of 50 unit cells. A transverse edge displacement excitation is prescribed on the left end middle edge while the right end middle edge is fixed.

Results

Frequency response analysis

A range of 0-1000 Hz is selected to keep consistent with the dispersion analyses. In Figure 7 and 8 the frequency response functions of the transverse displacement at $2/5$ and $4/5$ of the finitely long 3D and 2D LRAM panel are displayed. For the purpose of reference, results of the host panel (a panel consisting only of the matrix glass material) are added. The band gap obtained from dispersion analyses is highlighted in green, it fits well with the anti-resonances at both gauge points. What also can be seen is that there is hardly any difference between the frequency response of the 3D and 2D LRAM panel, as expected. The same applies to the host panel.

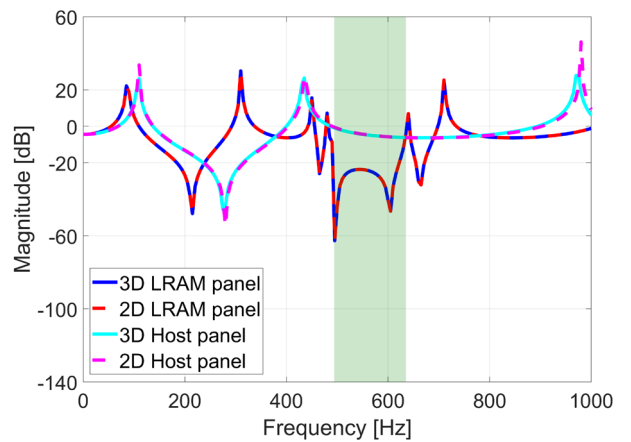


Figure 7: The transverse displacement frequency responses at $2/5$ of the finitely long 3D and 2D LRAM/host panels. The band gap obtained from dispersion analyses is highlighted in green.

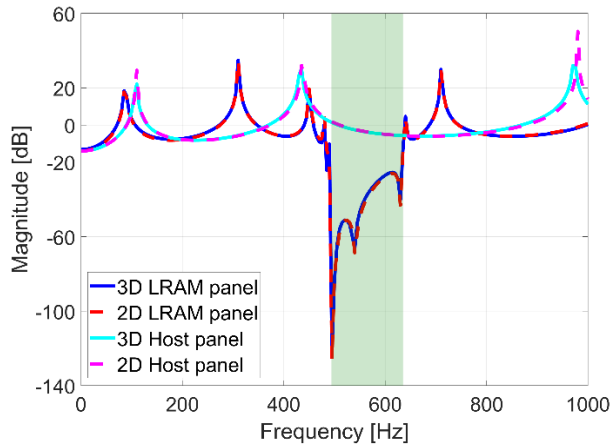


Figure 8: The transverse displacement frequency responses at 4/5 of the finitely long 3D and 2D LRAM/host panels. The band gap obtained from dispersion analyses is highlighted in green.

To give a more comprehensive comparison between 3D and 2D LRAM panels the frequency response transverse displacement distributions of the finitely long 3D and 2D LRAM are plotted for three frequencies in Figure 9(a). The corresponding deformed boundaries of the 3D LRAM panel are displayed in Figure 9(b). The first frequency is chosen below the band gap at 250 Hz. As expected, locally resonant effects are not functioning and the displacement along the panel is large, it behaves as a host panel. The second frequency is chosen in the band gap at 500 Hz. Clear wave attenuation is visible, the flexural wave propagates until approximately 0.1 m ($10L_m$), the other unit cells are unmoved. The other frequency is chosen at 750 Hz where there is no localized resonant effect. As seen, the wave is free to propagate through the panel. Figure 7, 8 and 9 show that the 3D LRAM panel consisting of unit cells with width $W_m = 10L_m$ indeed produces the same frequency response results as the 2D LRAM panel.

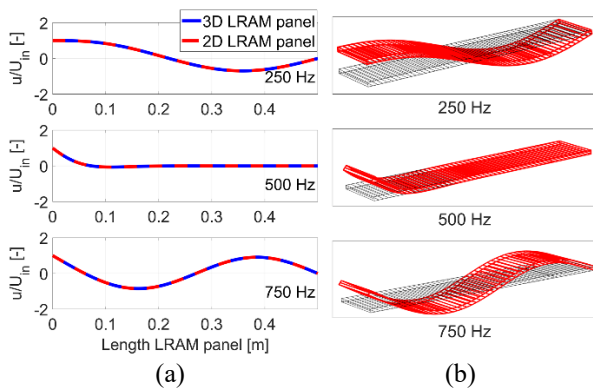


Figure 9: The (a) transverse displacement amplitude distributions on the finitely long 3D and 2D LRAM panels, at three different frequencies, and (b) associated full-scale deformation modes of 3D LRAM panel. The deformation is magnified by a factor 40.

CONCLUSION

This paper elaborately compares 3D and 2D modelling approaches for a typical LRAM panel with the consistent along-width cross-section, through dispersion and frequency response analyses on a typical design. The following conclusions are highlighted:

- For the infinitely long 3D LRAM panels with consistent along-width cross-section, 2D simplification modelling can be regarded as sufficient if the unit cell width-to-length ratio is over 10. Furthermore, if the width-to-length ratio is over 10 for 3D LRAM panels with finite length, the frequency response in the subwavelength range of 3D and 2D LRAM panels can be considered identical.

In order to achieve more general conclusions, further work can be carried out on LRAM panels with negative effective modulus or double negative effects and also those with intricate geometries, e.g. cylindrical shells.

ROLE OF THE STUDENT

Henok Abadi was an undergraduate student at Eindhoven University of Technology supervised by ir. Lei Liu and dr.ir. Varvara Kouznetsova, when the research in this paper was performed. The topic was proposed by the supervisors. Numerical simulations, analysis of results, conclusions and writing of the research paper were done by the student.

ACKNOWLEDGMENTS

I would like to thank ir. Lei Liu, who was very willing to answer my questions and give helpful feedback.

REFERENCES

1. Zheng, X. et al. (2014). Ultralight, ultrastiff mechanical metamaterials. *Science*, 334(6190):1373-1377.
2. Bein, T. et al. (2012). Integrated solutions for noise and vibration control in vehicles. *Procedia - Social and Behavioral Sciences*, 48:919-931.
3. Qin, Y., Hornikx, M. C. J., Bron, S., & Koopman, A. (2017). Laboratory experiments and modal model of impact sound transmission through a lightweight wooden floor. In *24th International Congress on Sound and Vibration, ICSV 2017* International Institute of Acoustics and Vibration (IIAV).
4. Gusev, V. E., & Wright, O. B. (2014). Double-negative flexural acoustic metamaterial. *New Journal of Physics*, 16(12):123053.
5. Nateghi, A. et al. (2016). Wave propagation in locally resonant cylindrically curved metamaterial panels. *International Journal of Mechanical Sciences* 127. 73-79.
6. Liu, L. (2018). A general homogenization method for LRAM panels (Master thesis, Eindhoven University of Technology)
7. Liu, Z. et al. (2000). Locally Resonant Sonic Materials. *Science*, 289(5485), 1734 LP-1736.
8. Makishima, A., & Mackenzie, J. D. (1975). Calculation of Bulk Modulus, Shear Modulus and Poisson's Ratio of Glass. *Journal of Non-Crystalline Solids*. 17. 147-157. 10.1016/0022-3093(75)90047-2.
9. Markidou, A., Shih, W. Y., & Shih, W. (2005). Soft-materials elastic and shear moduli measurement using piezoelectric cantilevers. *Review of Scientific Instruments* 76, 064302.
10. Krushynska, A. O., Kouznetsova, V., & Geers, M. G. D. (2014). Towards optimal design of locally resonant acoustic metamaterials. *Journal of the Mechanics and Physics of Solids*, 71(1), 179-196.
11. Hussein, M., Leamy, M., & Ruzzene, M. (2014). Dynamics of Phononic Materials and Structures: Historical Origins, Recent Progress, and Future Outlook. *ASME Appl. Mech. Rev.*, 66(4), p. 040802